Heart Vessels (2013) 28:66–75
DOI 10.1007/s00380-011-0217-2

ORIGINAL ARTICLE

Assessment of vascular remodeling after the Fontan procedure using a novel very high resolution ultrasound method: arterial wall thinning and venous thickening in late follow-up

Taisto Sarkola · Edgar Jaeggi · Cameron Slorach · Wei Hui · Timothy Bradley · Andrew N. Redington

Received: 5 September 2011 / Accepted: 4 November 2011 / Published online: 14 February 2012

Abstract The Fontan circulation is associated with an increased central venous pressure, decreased ventricular preload, and increased afterload. We postulated that these central hemodynamic abnormalities would have consequences for the structural and functional properties of the peripheral arteries and veins, and performed a cross-sectional study in a tertiary health-care setting. We prospectively examined venous and arterial wall morphology by very high resolution ultrasound (VHRU, 25–55 MHz), and function by conventional vascular ultrasound (flow-mediated dilatation, FMD) and applanation tonometry (pulse wave velocity, PWV) in 28 patients after the Fontan procedure (age 14.8 ± 1.3 years) and 54 age-matched controls. Pig venous samples were studied with VHRU and compared with histology for accuracy. The precision of the venous VHRU method was studied in healthy volunteers. The lumen dimension was reduced in Fontans compared with controls in the common carotid, brachial, radial, and femoral arteries ($p < 0.05$). The common carotid, brachial, radial, ulnar, femoral, and dorsal tibial artery intima-media thicknesses (IMTs) and the brachial, ulnar, and femoral artery adventitial thicknesses were decreased ($p < 0.05$ for all), while the cubital and dorsal tibial vein IMTs were increased in Fontans ($p < 0.001$). FMD, abdominal aortic stiffness, and carotid-femoral PWV were similar, while carotid-radial artery PWV was increased in Fontans ($p < 0.01$). Venous wall layer assessment with VHRU was accurate and precise. The Fontan circulation is associated with significant arterial and venous remodeling, presumably reflecting abnormalities of central hemodynamics. These novel data may be of clinical importance in the circulatory management as well as the understanding of the early pathogenesis of vasculopathy in patients after the Fontan procedure.

Keywords Artery wall morphology · Vein wall morphology · Intima-media thickness · Vascular stiffness · Fontan circulation

Abbreviations

AT	Adventitia thickness
BP	Blood pressure
CV	Coefficient of variation
FMD	Flow-mediated dilatation
IMT	Intima-media thickness
IMAT	Intima-media-adventitia thickness
LD	Lumen dimension
PWV	Pulse wave velocity
VHRU	Very high resolution ultrasound
VO_2	Oxygen consumption

Electronic supplementary material The online version of this article (doi:10.1007/s00380-011-0217-2) contains supplementary material, which is available to authorized users.

T. Sarkola · E. Jaeggi · C. Slorach · W. Hui · T. Bradley · A. N. Redington (✉)
Division of Cardiology, Labatt Family Heart Centre, The Hospital for Sick Children, University of Toronto, 555 University Avenue, Toronto, ON M5G 1X8, Canada
e-mail: andrew.redington@sickkids.ca

T. Sarkola
e-mail: taisto.sarkola@helsinki.fi

T. Sarkola
Division of Cardiology, Helsinki University Central Hospital for Children and Adolescents, POB 281, 00029 Helsinki, Finland

E. Jaeggi · A. N. Redington
Research Institute, The Hospital for Sick Children, University of Toronto, Toronto, Canada

Introduction

With the development of the Fontan operation [1] and its subsequent modifications [2–4], more and more patients with single ventricles are surviving into adulthood. Despite improvements in early outcomes, there is time-dependent attrition and increasing cardiovascular morbidity [5]. The factors that contribute to the hemodynamic compromise are, however, still incompletely understood. The Fontan circulation is necessarily abnormal, with a chronically low cardiac output state [6], ventricular diastolic dysfunction [7], abnormal peripheral hemodynamics [8], and with the circulation described as afterload impaired and preload challenged [9]. Despite these data concentrating on the systemic circulation, the pulmonary vascular bed may be a key component in the overall circulatory disturbance. The absence of a subpulmonary pumping chamber imposes an elevated central venous pressure that is transmitted to the abdominal organs and peripheral venous and lymphatic systems, which is thought to contribute to chronic venous insufficiency in the lower extremity [10] as well as to more serious conditions such as liver cirrhosis [11], protein-losing enteropathy, [12] and plastic bronchitis [13].

The effect of these central hemodynamic abnormalities on arterial and venous properties has come under scrutiny. Increased carotid intima-media thickness (IMT) [14], peripheral endothelial dysfunction, reduced venous compliance, increased microvascular filtration pressures and threshold for edema, and higher arterial resistance in the lower extremity have been reported in post-Fontan adolescents [8, 15, 16].

Despite these physiologic observations, the peripheral arterial and venous wall morphology in patients that have adapted to the Fontan circulation is largely unknown. We have recently validated a noninvasive very high resolution ultrasound (VHRU) method to assess the combined intima-media, adventitia, and total wall thicknesses of superficial elastic and muscular arteries using 25–55 MHz transducers [17], and we have reported on its use in adolescents with congenital and acquired cardiovascular conditions [18, 19]. In this study, we validated the VHRU method for the assessment of peripheral venous wall layers. This allowed us to study the arterial and venous wall morphology in detail in conjunction with functional vascular testing in adolescents that have adapted to the Fontan circulation in comparison to an age-matched control group. The hypothesis was that the Fontan circulation is associated with remodeling of the peripheral arteries and veins.

Methods

The study was conducted in accordance with the Declaration of Helsinki, approved by the Institutional Research Ethics Board and Health Canada, and participation required written informed consent.

Study design and populations

This was a prospective cross-sectional study. Twenty-eight out of 31 consecutive Fontan patients aged 12–17 (14.8 ± 1.3) years attending the echocardiography laboratory at the Hospital for Sick Children, Toronto, between November 2009 and early June 2010 consented to participate in the study. None of the patients had a known chromosomal abnormality, diabetes or a lipid disorder requiring medication, or admitted smoking. One patient had the VACTERL association with a previously operated trachea-esophageal fistula. All of the patients had undergone completion of the Fontan procedure with a fenestrated extracardiac conduit. The fenestration had been closed with a device in 23 out of 28 patients, and spontaneous closure was confirmed by echocardiography in the rest. None of the Fontans were in significant heart failure, and they were all hemodynamically compensated and in relatively good clinical condition. Peak workload, peak VO_2 (oxygen consumption), and percent of predicted peak VO_2 and VO_2 at the anaerobic threshold of the patient's most recent clinical exercise tests were, in addition to the use of medication, retrospectively reviewed from hospital records. Twenty-one patients had undergone bicycle ergometry and four patients treadmill exercise tests using the Bruce protocol within the preceding 2 years (median 0.5, range 0–2 years). The characteristics are shown in Table 1.

The arterial measurements were compared with data from a healthy age-matched control group of 54 subjects without medications who had been recruited from nearby schools or referred to the hospital for the assessment of an innocent murmur. In addition, 32 age-matched (14.8 ± 3.1 years) subjects with no abnormal venous hemodynamics or diastolic dysfunction on standard echocardiography were recruited as controls for peripheral venous imaging.

All measurements were obtained in the supine position after at least 30 min of rest in the echo laboratory at the Hospital for Sick Children, Toronto. Height was measured with a stadiometer, weight with an electronic balance, oxygen saturation with a pulse oximeter, and blood pressure (BP) with an oscillometric device (Dinamap, Critikon Inc.) during simultaneous echocardiographic and vascular imaging [20]. Reliability assessments of the different methods were made on healthy personnel.

Vascular morphology imaging

Ultrasound recordings from peripheral muscular arteries were obtained using the Vevo 770 ultrasound system

Table 1 Clinical characteristics of controls and Fontan patients

N:	Control 54	Fontan 28	*p* value
Age (years, mean ± SD)	14.8 ± 1.6	14.8 ± 1.3	NS
Height (cm)	165 ± 11	160 ± 10	<0.05
Weight (kg)	58.8 ± 14.9	53.0 ± 12.2	NS
BMI (kg/m^2)	21.3 ± 3.8	20.4 ± 3.1	NS
BMI *z* score	0.20 ± 0.99	-0.03 ± 1.14	NS
Gender (males/females)	34/20	15/12	NS
Right arm SBP	107 ± 9	101 ± 10	<0.05
Right arm DBP	53 ± 6	53 ± 9	NS
Left arm SBP	106 ± 9	103 ± 12	NS
Left arm DBP	56 ± 5	56 ± 9	NS
Left thigh SBP	112 ± 11	116 ± 15	NS
Left thigh DBP	44 ± 5	45 ± 7	NS
Saturation (%)	99[f]	95 ± 2	<0.001
Cardiac diagnosis			
Aortic/pulmonary outflow obstruction at birth		9/16	
Pulmonary atresia		11	
Hypoplastic left heart syndrome		5	
Double inlet left or right ventricle		3	
Other single ventricle		9	
Fontan procedure			
Surgical palliation in three stages[a]		24	
Extracardiac conduit with fenestration		28	
Age at Fontan completion (years, median, range)		2.8 (1.3–11.7)	
Treatments			
ACE inhibition[b]		14	
Anticoagulation[c]		13	
β-Blocker[d]		4	
Digoxin		3	
Pacemaker		5	
Fontan morbidities			
PLE or liver cirrhosis		2	
Recent exercise test results			
Peak workload (W)		96 ± 31	
% of predicted peak workload		61 ± 11	
Peak VO_2 (ml/kg/min)		29 ± 7	
Peak VO_2% of predicted		67 ± 14	
VO_2 anaerobic threshold (ml/kg/min)[e]		26 ± 7	
% of predicted VO_2 anaerobic threshold		78 ± 21	

Blood pressures are in mmHg

In addition, one Fontan patient with PLE reported long-term use of hydrochlorothiazide and spironolactone

BSA body surface area, *BMI* body mass index, *SBP* systolic blood pressure, *DBP* diastolic blood pressure

[a] Norwood or DKS with or without shunt or pulmonary artery banding, bidirectional cavopulmonary shunt, total extracardiac cavopulmonary shunt

[b] Includes long-term use of enalapril in 8, ramipril in 4, and fosinopril in 2

[c] Includes long-term use of aspirin in 12, warfarin in 1, and both aspirin and warfarin in 1

[d] Includes long-term use of atenolol in 3 and nadolol in 1

[e] $N = 15$, anaerobic threshold not reached in 4 patients and not determined in 6 patients

[f] Saturation assumed, not measured

(Visualsonics, Toronto, Canada) with mechanical 25 MHz (RMV710B), 35 MHz (RMV712), and 55 MHz (RMV708) linear transducers, and stored for off-line analysis. Care was taken not to compress the vessels during image acquisition.

The radial and ulnar arteries were studied 1–2 cm proximal to the skin fold that separates the palma manus from the anterior antebrachial region, the anterior tibial artery proximal to the first metatarsal bone, the dorsal tibial artery at the medial malleolar level, the common carotid artery 1 cm proximal to the carotid bulb, the brachial artery 2 cm proximal to the cubital skin fold, and the common femoral artery at the inguinal skin fold. The cubital vein was imaged at the cubital skin fold and the dorsal tibial vein at the medial malleolar level. The largest vein in the region was chosen. The 35 MHz transducer was used to determine the lumen dimension (LD) of the uncompressed vein and the 55 MHz transducer applied to study the venous far-wall morphology. Both right and left vessels were imaged.

Offline measurements of coded high-quality vascular images showing a good distinction between structural interfaces were performed manually by a single investigator (TS) blinded to the clinical data with electronic calipers in a very high-resolution zoom window (Vevo 770 software, version 2.3.0). The combined end-diastolic IMT and intima-media-adventitia thickness (IMAT) were measured from the far wall with the leading edge technique, and the end-diastolic and peak-systolic (carotid only) LDs were measured with reference to the simultaneously recorded electrocardiogram. Adventitia thickness (AT) was calculated as the difference between IMT and IMAT. We have recently reported arterial method validation, accuracy, and precision [17]. The intra- and interobserver and the test–retest CVs for arterial IMT were in the range 7–9% ($N = 44$–113) for 25 MHz, in the range 9–19% ($N = 25$–65) for 35 MHz, and in the range 11–16% ($N = 43$–114) for 55 MHz. The intra- and interobserver and the test–retest CVs for arterial IMAT were in the range 5–8% ($N = 40$–112) for 25 MHz, in the range 8–11% ($N = 24$–65) for 35 MHz, and in the range 14–15% ($N = 41$–112) for 55 MHz. The intra- and interobserver and the test–retest CVs for the calculated arterial AT were in the range 15–19% ($N = 38$–111) for 25 MHz, in the range 20–25% ($N = 23$–65) for 35 MHz, and in the range 20–22% ($N = 39$–112) for 55 MHz.

Venous imaging accuracy

Transcutaneous VHRU has not been validated to examine veins. For accuracy, wall measurements on 1–2 cm venous specimens of the inferior vena caval, internal jugular, subclavian, renal, and femoral veins were, therefore, obtained within 2 h post mortem from 6 pigs (weight about 35 kg) to obtain a range of different vessel structures and sizes. The specimens were tied on catheters, fixed in buffered (1:10) formalin for at least 24 h, and imaged in long and short axis sweeps with 55 MHz. A negligible shrinkage of 1% was noted for IMAT ($N = 8$). Gain settings were optimized to minimize the amount of scatter and to produce a sharp distinction between the different layers. Venous IMT and IMAT were defined as the distance between the lumen–vessel interface and the external border of the echolucent zone and the distance between the lumen–vessel interface and the external vessel wall border, respectively [17, 21, 22]. Each specimen was cut in cross-section, embedded in paraffin, sectioned, and stained with elastic (Verhoeff's) trichrome. Anatomical orientation of the vessel was matched to the corresponding long and short axis ultrasound image, and the thickness of IMT and IMAT was measured at least 1 week after the ultrasound measurements using a Leica EZ4D stereomicroscope (Spectronic Analytical Instruments) with 20× or 30× magnification.

Arterial stiffness and endothelial function assessments

Carotid artery stiffness was calculated using the formula: stiffness index $\beta = \ln(\text{SBP}/\text{DBP})/((\text{LDs} - \text{LDd})/\text{LDd})$, where SBP is systolic BP, DBP is diastolic BP, LDs is systolic lumen dimension, and LDd diastolic lumen dimension [23]. Abdominal aortic stiffness was assessed in a similar manner to that previously described [24], but with M-mode using the Vivid 7 ultrasound system and EchoPAC (GE Medical Systems, Horten, Norway). The intra- and interobserver and the test–retest CVs for the carotid stiffness index were 15, 17, and 22%, respectively ($N = 27$). The intra- and interobserver and the test–retest CVs for the end-diastolic abdominal aortic lumen diameter were 4% ($N = 19$), 4% ($N = 19$), and 3% ($N = 9$), respectively, and for aortic stiffness index 25, 26, and 37%, respectively ($N = 10$).

Pulse wave velocity (PWV) was assessed by sequentially recording ECG-gated right carotid and right radial artery and right carotid and right femoral artery waveforms with a high-fidelity micromanometer (SphygmoCor, AtCor Medical Systems Inc., Sydney, Australia) [25–27]. The intra- and interobserver and the test–retest CVs were 4% ($N = 20$), 14% ($N = 10$), and 14% ($N = 10$) for right carotid to right radial PWV, and 4% ($N = 20$), 17% ($N = 10$), and 9% ($N = 10$) for right carotid to right femoral PWV.

The flow-mediated dilatation (FMD) assessment was performed at the end of the study schedule following at least 4 h of fasting and more than 1 h of resting in the supine position [28]. FMD was assessed with the Vivid 7 system equipped with a 12 MHz transducer attached to a stereotactic probe-holding device using an automatic edge-

detection algorithm (Vascular Tools, Medical Imaging Applications, Coralville, IA, USA) to acquire longitudinal, ECG-gated, end-diastolic images of the right brachial artery 3–5 cm above the antecubital fossa every 3 s. Images were recorded for 1 min baseline, during 5 min pressure cuff inflation to >200 mmHg around the forearm, and for 5 min after cuff deflation. We were able to obtain adequate imaging in 49/54 controls and 21/28 Fontans due to lack of cooperation or consent in some study subjects. The intra- and interobserver and the test–retest CVs for FMD were 26% ($N = 19$), 38% ($N = 19$), and 43% ($N = 9$).

Data analysis

Descriptive statistics are reported as mean ± SD or median (range) for continuous variables and as percentages for categorical variables. BMI z scores were derived based on Centre for Disease Control (CDC) growth charts [29]. The relationship between histology- and VHRU-derived venous measurements was assessed with the Pearson correlation coefficient and the degree of agreement was calculated [30]. The average of left and right vessel measurements is reported (no difference). Student and paired t tests were used as appropriate. Univariate and multiple linear regression analyses were performed, with diagnosis of Fontan, male gender, and use of medications entered as nominal (0 or 1) and all other measures as continuous variables (PASW Statistics 18, SPSS Inc., Chicago, IL, USA).

Results

Reliability and accuracy of venous layer thickness measurements

The venous IMT was identified by light microscopy in 40 of the 45 samples and by VHRU in 21 of the 45 samples (due to limited VHRU resolution at <0.05 mm), with a good correlation between histologically and 55 MHz-derived IMT ($r = 0.87$, $p < 0.001$, range 0.01–0.21 mm) (Fig. 1). Agreement analysis of these 21 samples showed a mean difference of 0.004 mm, equal to 4% of the mean (NS for bias), 95% limits of agreement −0.058 to 0.065, and CV 38%. The venous IMAT was identified by light microscopy and by VHRU in all 45 samples, with a good correlation between histology and 55 MHz ($r = 0.84$, $p < 0.001$, range 0.05–0.35 mm). Agreement analysis for these 45 samples with IMAT showed a mean difference of 0.030 mm, equal to 17% of the mean (NS for bias), 95% limits of agreement −0.067 to 0.133, and CV 24%. The intra- and interobserver and the test–retest CVs for venous IMT were 12 and 13, 12 and 15, and 26 and 27% with the 35 and 55 MHz probes, respectively ($N = 39$). The intra- and interobserver and the test–retest CVs for venous IMAT were 16 and 16, 17 and 12, and 20 and 25% with the 35 and 55 MHz probes, respectively ($N = 44$).

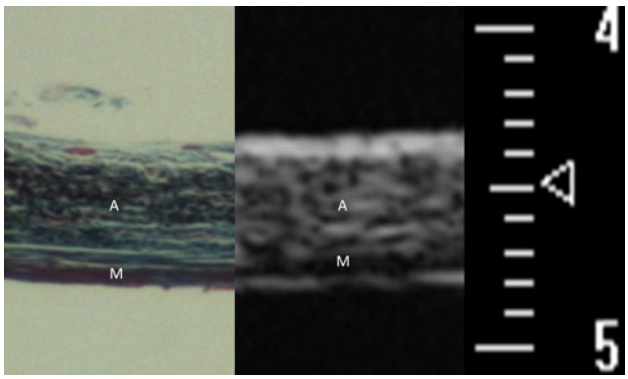

Fig. 1 Histology versus VHRU for venous wall morphology. The figure shows the histology of a pig inferior caval vein specimen compared with the VHRU image obtained with the 55 MHz probe. The vein displays a pattern consistent with the echolucent muscular media (*M*) and the relatively thick and echodence adventitia (*A*) containing mainly connective tissue. Histological staining for muscle in *red*, elastin in *black*, and collagen in *green*. The scale is in millimeters (color figure online)

Arterial lumen dimensions and wall layer thickness

The characteristics of the controls and Fontans are shown in Table 1. The right arm systolic BP was lower among Fontans compared with controls. The common carotid, brachial, radial, and femoral arterial LDs were reduced in Fontans. Carotid, brachial, radial, ulnar, femoral, and dorsal tibial artery IMTs were all thinner in Fontans (Table 2; Fig. 2). Thinner AT was observed in brachial, ulnar, and femoral arteries of Fontans.

Regional systolic BP, BMI, age, and gender were all significantly and positively associated with most arterial site IMT and LD measurements (see the Electronic supplementary material, ESM, Tables 4a, 4b, and 4c). After adjustments, the diagnosis of Fontan remained significant for carotid LD, brachial LD and IMT, radial IMT, ulnar IMT, and femoral IMT and LD. Regional BP remained significant for carotid IMT, femoral AT, and dorsal tibial LD. BMI remained significant for carotid LD, brachial LD, radial LD, and anterior tibial LD. Age remained significant for brachial IMT and LD, ulnar LD, and femoral IMT and LD. Male gender remained significant for carotid LD, brachial IMT and LD, radial IMT and LD, ulnar IMT, and dorsal tibial IMT.

A subanalysis including Fontans only ($N = 28$) was performed regarding the long-term use of ACE inhibition or anticoagulation ($N = 14$ and 13, respectively), resting

Table 2 Arterial morphology and function in controls and Fontan patients

N:	Control 54	Fontan 28	*p* value
Common carotid IMT (mm)	0.410 ± 0.058	0.379 ± 0.052	<0.05
Common carotid LD (mm)	5.36 ± 0.44	5.02 ± 0.51	<0.01
Common carotid stiffness index	4.29 ± 1.12	3.85 ± 0.95	NS
Brachial IMT (mm)	0.163 ± 0.025	0.130 ± 0.022	<0.001
Brachial AT (mm)	0.133 ± 0.023	0.123 ± 0.020	<0.05
Brachial LD (mm)	2.95 ± 0.51	2.67 ± 0.47	<0.05
Radial IMT (mm)	0.145 ± 0.022	0.130 ± 0.028	<0.01
Radial AT (mm)	0.078 ± 0.016	0.079 ± 0.013	NS
Radial LD (mm)	1.73 ± 0.28	1.59 ± 0.27	<0.05
Ulnar IMT (mm)	0.193 ± 0.030	0.170 ± 0.037	<0.01
Ulnar AT (mm)	0.091 ± 0.019	0.084 ± 0.011	<0.05
Ulnar LD (mm)	1.52 ± 0.36	1.61 ± 0.35	NS
Femoral IMT (mm)[a]	0.264 ± 0.054	0.231 ± 0.056	<0.05
Femoral AT (mm)[a]	0.237 ± 0.058	0.253 ± 0.069	<0.05
Femoral LD (mm)[a]	6.62 ± 1.11	5.47 ± 0.84	<0.001
Anterior tibial IMT (mm)	0.155 ± 0.030	0.145 ± 0.025	NS
Anterior tibial AT (mm)	0.090 ± 0.018	0.087 ± 0.014	NS
Anterior tibial LD (mm)	1.32 ± 0.44	1.38 ± 0.31	NS
Dorsal tibial IMT (mm)	0.251 ± 0.044	0.230 ± 0.046	NS
Dorsal tibial AT (mm)	0.112 ± 0.024	0.106 ± 0.031	NS
Dorsal tibial LD (mm)	1.76 ± 0.40	1.65 ± 0.43	NS
Abdominal aorta LD (mm)[d]	11.9 ± 2.2	11.2 ± 2.7	NS
Abdominal aorta stiffness index	3.18 ± 1.05	3.58 ± 2.23	NS
Right carotid-femoral PWV (m/s)[b]	5.0 ± 1.0	5.2 ± 1.1	NS
Right carotid-radial PWV (m/s)	6.3 ± 1.0	7.4 ± 1.7	<0.01
FMD (% change)[c]	8.6 ± 4.2	8.0 ± 3.5	NS
FMD time to peak dilatation (s)	43 ± 14	48 ± 22	NS

The means of right and left artery layer thicknesses and dimensions are reported

IMT intima-media thickness, *AT* adventitia thickness, *LD* lumen dimension in end diastole, *PWV* pulse wave velocity, *FMD* flow-mediated dilatation

[a] $N = 27$ controls and 22 Fontans

[b] $N = 52$ controls and 23 Fontans

[c] $N = 49$ controls and 21 Fontans

[d] $N = 52$ controls and 17 Fontans

oxygen saturation, and time since Fontan completion. Use of ACE inhibitors was associated with a lower systolic (108 ± 9 vs. 98 ± 13 mmHg, $p < 0.05$) and diastolic (60 ± 7 vs. 51 ± 7 mmHg, $p < 0.01$) BP. We were unable to detect any significant associations between any of the arterial layer thicknesses or LDs and the use of ACE inhibitor, anticoagulation, resting oxygen saturation, or exercise test parameters. Time since Fontan completion was negatively associated with carotid ($r = -0.36$, $p < 0.05$) and radial ($r = -0.46$, $p < 0.05$) artery LDs, but not with other layer thickness or LDs, and these associations remained significant when adjusting for age, BMI, and gender with multiple regression analyses.

Arterial stiffness and endothelial function

No difference was observed in abdominal aortic and carotid artery stiffness indices and in carotid to femoral PWV between Fontans and controls (Table 2). The right carotid to right radial PWV was significantly higher in Fontans. This association remained significant when adjusting for age, BMI, gender, regional BP or carotid, and brachial or radial artery LD. Brachial artery IMT, AT, or LD was not associated with carotid to radial PWV. FMD and FMD time to peak dilatation were not different in Fontans (Table 2). No significant association between right carotid to right radial PWV or FMD and the use of ACE inhibitors,

anticoagulation, resting oxygen saturation, peak VO_2 or percent of predicted peak VO_2, or time since Fontan completion was observed among Fontans.

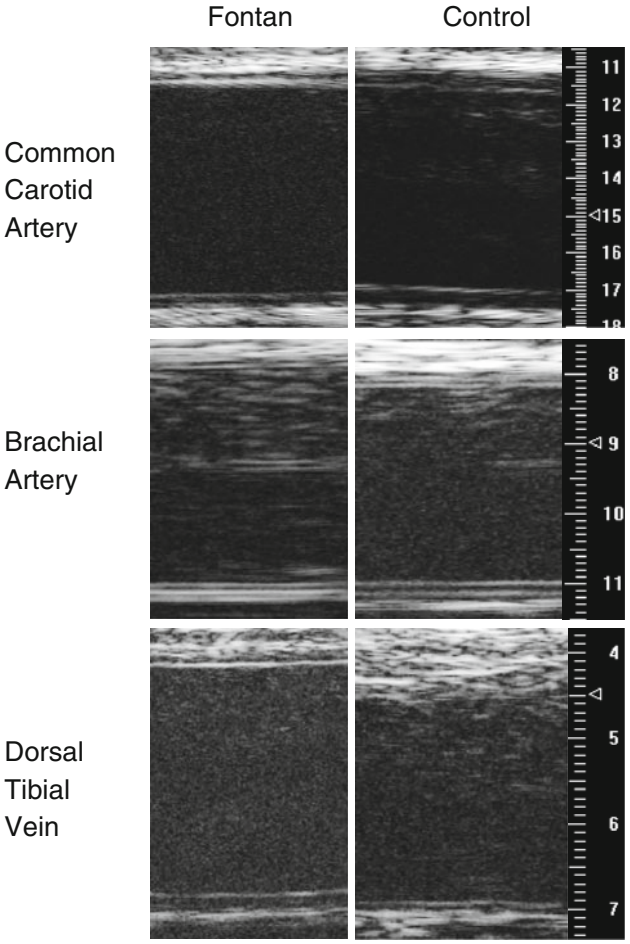

Fig. 2 In vivo VHRU in a Fontan patient and controls. In vivo transcutaneous VHRU of the common carotid artery (25 MHz), brachial artery (35 MHz), and dorsal tibial vein (55 MHz) in a 15-year old Fontan patient and control. The scale is in millimeters. The arterial walls (IMT and AT) are thin and the venous wall shows thickening of the echolucent media in the Fontan patient

Venous lumen dimensions and wall layer thickness

Venous LDs were not different between Fontans and controls. In contrast, both the upper arm cubital vein and lower leg dorsal tibial vein IMTs were increased in Fontans (Table 3; Fig. 2). The cubital vein IMT was thicker than the dorsal tibial vein IMT in both Fontans ($p < 0.001$) and controls ($p < 0.001$). BMI was positively associated with dorsal tibial vein IMT and IMAT. The differences in venous IMT and IMAT between the Fontans and controls remained significant when adjusting for age, BMI, and gender (ESM Table 4d).

In a subanalysis including Fontans only ($N = 28$), long-term use of ACE inhibition ($N = 14$) was associated with a decreased dorsal tibial vein IMAT (0.216 ± 0.039 vs. 0.256 ± 0.057 mm, $p < 0.05$), but no associations with other venous measurements were found. A similar decrease was observed regarding long-term use of anticoagulation ($N = 13$) for dorsal tibial vein IMAT (0.209 ± 0.032 vs. 0.259 ± 0.056 mm, $p < 0.001$) and cubital vein IMT (0.079 ± 0.016 vs. 0.096 ± 0.019 mm, $p < 0.05$), with no associations with other venous measurements. These remained significant when adjusting for age, BMI, and gender. No significant association between resting oxygen saturation, time since Fontan completion, or exercise test parameters and venous measurements was found.

Discussion

This is the first study to use VHRU to examine the peripheral vascular properties of Fontans. We show that VHRU is able to assess the venous wall morphology in almost microscopical detail. Indeed, the results of the current study show important and hitherto undescribed evidence of both arterial and venous remodeling as a consequence of the Fontan circulation. In short, Fontans displayed small and thin peripheral arteries as well as thick peripheral veins.

Table 3 Venous lumen dimension and layer thickness in controls and Fontan patients

	Control	Fontan	*p* value
N:	32	28	
Cubital vein IMT (mm)	0.072 ± 0.015	0.089 ± 0.020	<0.001
Cubital vein IMAT (mm)	0.188 ± 0.037	0.200 ± 0.042	NS
Cubital vein LD (mm)	3.42 ± 0.96	3.05 ± 0.87	NS
Dorsal tibial vein IMT (mm)	0.102 ± 0.022***	0.136 ± 0.038***	<0.001
Dorsal tibial vein IMAT (mm)	0.206 ± 0.031	0.236 ± 0.052	<0.01
Dorsal tibial vein LD (mm)	2.45 ± 0.47	2.49 ± 0.56	NS

The means of right and left veins are reported

IMT intima-media thickness, *IMAT* intima-media-adventitia thickness, *LD* lumen dimension in end diastole

*** $p < 0.001$ compared with cubital vein IMT

The key feature of the modern iterations of the Fontan circulation is the rerouting of the systemic venous return directly to the pulmonary arteries without a subpulmonary pumping chamber. This necessarily imposes major alterations on the central venous pressure and the flow dynamics in the pulmonary vascular bed; as a consequence, it is usually associated with reduced preload to the single ventricle. The venous IMT thickening observed in our Fontans is well in line with the general principles of the Fontan circulation and is likely related to the thickening of the muscular media layer in response to increased venous pressure and wall stress, as our previous and present validations of the IMT show that the intima thickness of the intima-media complex represents <5% in nonatherogenic vessels [17]. The difference between upper and lower extremity venous IMT is also consistent with the difference in the peripheral venous pressure related to the weight of the column of blood between the heart and the ankle, albeit exaggerated in Fontans. These results are in line with recent studies showing venous stiffening in adolescent Fontans [8], as well data documenting a high frequency of chronic venous insufficiency in Fontans during young adulthood [10].

Our finding that chronic ACE inhibition (and anticoagulation) modulated venous remodeling in the dorsal tibial vein (but no other venous or arterial sites) should be interpreted with caution. Although not designed to address the role of ACE inhibition, half of our Fontans received this therapy, primarily based on physician preference. This is in line with the frequency of use described in the cross-sectional study recently reported by the Pediatric Heart Network [31]. That data set showed no difference between those receiving and not receiving ACE inhibition, and overall we were unable to show any significant difference as a result of chronic ACE inhibition, perhaps suggesting that the arterial and venous changes are secondary phenomena, and not primary determinants of abnormal cardiovascular performance.

The consistently small and thin carotid, femoral, and upper arm peripheral conduit arteries are in contrast to previous studies showing an increased carotid artery IMT in Fontans [14], and are consistent with a decreased wall stress due to decreased volume and pressure loading of these vessels long term. The observation of a negative correlation between time since Fontan completion and LDs is also in line with the hypothesis. That is not to say that systemic vascular resistance is lower in Fontans, as it has been consistently shown to be elevated in previous studies [8, 9]. Instead, we suggest that the arterial remodeling we describe is secondary to decreased flow, and that the findings of increased resistance may therefore, at least in part, be related to a decreased total cross-sectional area of the vascular tree, consistent with our finding of a widespread and consistent reduction in arterial luminal diameter. Interestingly, these differences remained significant when adjusting for regional BP, body size, age and gender, suggesting that the arterial changes are indeed related to the chronically decreased volume load, flow, and cardiac output described in Fontans [6, 9].

The novel finding of increased vascular stiffness in the upper right arm, but not in the central aorta or carotid artery, of the Fontans is in contrast with recent vascular findings in tetralogy of Fallot [32], and perhaps counter-intuitive given the thinner arterial wall. However, the Moens–Korteweg equation for deriving PWV relates PWV directly to vessel wall thickness as well as to the reciprocal of vessel radius. This suggests that the changes in vessel diameter predominate over those of the arterial wall, at least in terms of PWV, although this is difficult to prove in the absence of direct measurement of the physical properties.

Finally, we were unable to demonstrate any difference in right brachial FMD. This is in contrast to previous reports showing diminished FMD responses [15, 16]. The FMD in our controls is, however, similar to that previously reported for healthy teenagers [33], and while the response among our Fontans was slightly lower, it was not statistically significant. Furthermore, none of the vascular parameters correlated with exercise performance in our cohort. The lack of a difference in FMD may be due to differences in the Fontan completion strategies applied, patient age, our relatively small sample size, and the influence of technical variability or preceding BP measurements [34].

This study has several limitations. Even if the VHRU accuracy is good for wall layer thickness overall, the arterial adventitial and venous IMTs of small peripheral vessels are, nevertheless, close to the limit of ultrasound resolution (0.03–0.05 mm) and challenged by some technical variability. Furthermore, the study included relatively young Fontans in good clinical condition, without significant heart failure or signs of chronic venous insufficiency or other significant hemodynamic morbidities. Only retrospective, although recent, exercise test data were included. The low number of Fontans with gastrointestinal morbidities precludes any conclusions relating to the vascular findings. On the other hand, we included a sufficient amount of age-matched healthy controls to optimize the statistical power. Our study included relatively young Fontans operated with the fenestrated extracardiac tunnel only, and may, therefore, not apply to older Fontans completed with other techniques. In the majority of the Fontans, the most recent invasive catheterization was performed more than a decade ago, precluding analyses in relation to invasive pressure data. Therefore, these results may only be applied to contemporary hemodynamically

stable young patients that have adapted to the Fontan circulation.

In conclusion, our results show significant changes in the morphology and size of the peripheral arteries and veins in adolescents that have adapted to the Fontan circulation. Further prospective studies are needed to clarify the role of these changes in the pathogenesis and the prediction of the development of significant hemodynamic morbidities in Fontans long term.

Acknowledgments Dr Jon Yeung is acknowledged for invaluable help in collecting the animal vessel samples, and Mrs. Huimin Wang for histological processing. The study was supported by grants from the Sigrid Juselius Foundation, the Instrumentarium Foundation, Societatis Medicorum Fennicae, the Finnish Cultural Foundation, the Finnish Foundation for Cardiovascular Research, and the Stockmann Foundation. The 25 and 35 MHz probes were loaned to the investigators by Visualsonics. The company had no other involvement in the study.

Conflict of interest None to declare.

References

1. Fontan F, Baudet E (1971) Surgical repair of tricuspid atresia. Thorax 26:240–248
2. de Leval MR, Kilner P, Gewillig M, Bull C (1988) Total cavopulmonary connection: a logical alternative to atriopulmonary connection for complex Fontan operations. Experimental studies and early clinical experience. J Thorac Cardiovasc Surg 96:682–695
3. Bridges ND, Lock JE, Castaneda AR (1990) Baffle fenestration with subsequent transcatheter closure. Modification of the Fontan operation for patients at increased risk. Circulation 82:1681–1689
4. Black MD, van Son JA, Haas GS (1995) Extracardiac Fontan operation with adjustable communication. Ann Thorac Surg 60:716–718
5. Khairy P, Fernandes SM, Mayer JE Jr, Triedman JK, Walsh EP, Lock JE, Landzberg MJ (2008) Long-term survival, modes of death, and predictors of mortality in patients with Fontan surgery. Circulation 117:85–92
6. Shachar GB, Fuhrman BP, Wang Y, Lucas RV Jr, Lock JE (1982) Rest and exercise hemodynamics after the Fontan procedure. Circulation 65:1043–1048
7. Olivier M, O'Leary PW, Pankratz VS, Lohse CM, Walsh BE, Tajik AJ, Seward JB (2003) Serial Doppler assessment of diastolic function before and after the Fontan operation. J Am Soc Echocardiogr 16:1136–1143
8. Krishnan US, Taneja I, Gewitz M, Young R, Stewart J (2009) Peripheral vascular adaptation and orthostatic tolerance in Fontan physiology. Circulation 120:1775–1783
9. Senzaki H, Masutani S, Ishido H, Taketazu M, Kobayashi T, Sasaki N, Asano H, Katogi T, Kyo S, Yokote Y (2006) Cardiac rest and reserve function in patients with Fontan circulation. J Am Coll Cardiol 47:2528–2535
10. Valente AM, Bhatt AB, Cook S, Earing MG, Gersony DR, Aboulhosn J, Opotowsky AR, Lui G, Gurvitz M, Graham D, Fernandes SM, Khairy P, Webb G, Gerhard-Herman M, Landzberg MJ, AARCC (Alliance for Adult Research in Congenital Cardiology) Investigators (2010) The CALF (Congenital Heart Disease in Adults Lower Extremity Systemic Venous Health in Fontan Patients) study. J Am Coll Cardiol 56:144–150
11. Kiesewetter CH, Sheron N, Vettukattill JJ, Hacking N, Stedman B, Millward-Sadler H, Haw M, Cope R, Salmon AP, Sivaprakasam MC, Kendall T, Keeton BR, Iredale JP, Veldtman GR (2007) Hepatic changes in the failing Fontan circulation. Heart 93:579–584
12. Mertens L, Hagler DJ, Sauer U, Somerville J, Gewillig M (1998) Protein-losing enteropathy after the Fontan operation: an international multicenter study. PLE study group. J Thorac Cardiovasc Surg 115:1063–1073
13. Costello JM, Steinhorn D, McColley S, Gerber ME, Kumar SP (2002) Treatment of plastic bronchitis in a Fontan patient with tissue plasminogen activator: a case report and review of the literature. Pediatrics 109:e67
14. Jin SM, Noh CI, Bae EJ, Choi JY, Yun YS (2007) Impaired vascular function in patients with Fontan circulation. Int J Cardiol 120:221–226
15. Mahle WT, Todd K, Fyfe DA (2003) Endothelial function following the Fontan operation. Am J Cardiol 91:1286–1288
16. Inai K, Saita Y, Takeda S, Nakazawa M, Kimura H (2004) Skeletal muscle hemodynamics and endothelial function in patients after Fontan operation. Am J Cardiol 93:792–797
17. Sarkola T, Redington AN, Keeley F, Bradley T, Jaeggi E (2010) Transcutaneous very high resolution ultrasound to quantify arterial wall layers of muscular and elastic arteries: validation of a method. Atherosclerosis 212:516–523
18. Sarkola T, Redington AN, Slorach C, Hui W, Bradley T, Jaeggi E (2011) Assessment of vascular phenotype using a novel very-high resolution ultrasound technique in adolescents after aortic coarctation repair and/or stent implantation: relationship to central hemodynamics and left ventricular mass. Heart 97:1788–1793
19. Sarkola T, Abadilla AA, Chahal N, Jaeggi E, McCrindle BW (2011) Feasibility of very-high resolution ultrasound to assess elastic and muscular arterial wall morphology in adolescents attending an outpatient clinic for obesity and lipid abnormalities. Atherosclerosis 219(2):610–615
20. Pickering TG, Hall JE, Appel LJ, Falkner BE, Graves J, Hill MN, Jones DW, Kurtz T, Sheps SG, Roccella EJ, Subcommittee of Professional, Public Education of the American Heart Association Council on High Blood Pressure Research (2005) Recommendations for blood pressure measurement in humans and experimental animals: part 1: blood pressure measurement in humans: a statement for professionals from the Subcommittee of Professional and Public Education of the American Heart Association Council on High Blood Pressure Research. Hypertension 45:142–161
21. Willard JE, Netto D, Demian SE, Haagen DR, Brickner ME, Eichhorn EJ, Grayburn PA (1992) Intravascular ultrasound imaging of saphenous vein grafts in vitro: comparison with histologic and quantitative angiographic findings. J Am Coll Cardiol 19:759–764
22. Hong MK, Mintz GS, Hong MK, Abizaid AS, Pichard AD, Satler LF, Kent KM, Leon MB (1999) Intravascular ultrasound assessment of the presence of vascular remodeling in diseased human saphenous vein bypass grafts. Am J Cardiol 84:992–998
23. Hirai T, Sasayama S, Kawasaki T, Yagi S (1989) Stiffness of systemic arteries in patients with myocardial infarction. A noninvasive method to predict severity of coronary atherosclerosis. Circulation 80:78–86
24. Vogt M, Kühn A, Baumgartner D, Baumgartner C, Busch R, Kostolny M, Hess J (2005) Impaired elastic properties of the ascending aorta in newborns before and early after successful coarctation repair: proof of a systemic vascular disease of the prestenotic arteries? Circulation 111:3269–3273

25. Bramwell JC, Hill AV (1922) Velocity of transmission of the pulse wave and elasticity of the arteries. Lancet 1:891–892
26. Rajzer MW, Wojciechowska W, Klocek M, Palka I, Brzozowska-Kiszka M, Kawecka-Jaszcz K (2008) Comparison of aortic pulse wave velocity measured by three techniques: Complior, SphygmoCor and Arteriograph. J Hypertens 26:2001–2007
27. Wilkinson IB, Fuchs SA, Jansen IM, Spratt JC, Murray GD, Cockcroft JR, Webb DJ (1998) Reproducibility of pulse wave velocity and augmentation index measured by pulse wave analysis. J Hypertens 16:2079–2084
28. Celermajer DS, Sorensen KE, Gooch VM, Spiegelhalter DJ, Miller OI, Sullivan ID, Lloyd JK, Deanfield JE (1992) Non-invasive detection of endothelial dysfunction in children and adults at risk of atherosclerosis. Lancet 340:1111–1115
29. Kuczmarski RJ, Ogden CL, Guo SS, Grummer-Strawn LM, Flegal KM, Mei Z, Wei R, Curtin LR, Roche AF, Johnson CL (2002) 2000 CDC Growth Charts for the United States: methods and development. National Center for Health Statistics. Vital Health Stat 11(246). http://www.cdc.gov/growthcharts/. Accessed 1 Sept 2010
30. Bland JM, Altman DG (1986) Statistical methods for assessing agreement between two methods of clinical measurement. Lancet 1:307–310
31. McCrindle BW, Williams RV, Mitchell PD, Hsu DT, Paridon SM, Atz AM, Li JS, Newburger JW, Pediatric Heart Network Investigators (2006) Relationship of patient and medical characteristics to health status in children and adolescents after the Fontan procedure. Circulation 113:1123–1129
32. László A, Pintér A, Horváth T, Kádár K, Temesvári A, Kollai M, Studinger P (2011) Impaired carotid artery elastic function in patients with tetralogy of Fallot. Heart Vessels 26:542–548
33. Järvisalo MJ, Rönnemaa T, Volanen I, Kaitosaari T, Kallio K, Hartiala JJ, Irjala K, Viikari JS, Simell O, Raitakari OT (2002) Brachial artery dilatation responses in healthy children and adolescents. Am J Physiol Heart Circ Physiol 282:H87–H92
34. Nerla R, Di Monaco A, Sestito A, Lamendola P, Di Stasio E, Romitelli F, Lanza GA, Crea F (2011) Transient endothelial dysfunction following flow-mediated dilation assessment. Heart Vessels 26:524–529